[redacted]

Copy

NASA TM X-477

NASA TM X-477

NASA TM X-477

TECHNICAL MEMORANDUM

X-477

COLD-AIR PERFORMANCE EVALUATION OF A THREE-STAGE TURBINE HAVING A BLADE-JET SPEED RATIO OF 0.156 DESIGNED FOR A 100,000-POUND-THRUST HYDROGEN-OXYGEN ROCKET TURBOPUMP APPLICATION

By Milton G. Kofskey

Lewis Research Center
Cleveland, Ohio

NATIONAL AERONAUTICS AND SPACE ADMINISTRATION

WASHINGTON November 1961

[redacted]

M

DECLASSI

[redacted]

E-1370

NATIONAL AERONAUTICS AND SPACE ADMINISTRATION

TECHNICAL MEMORANDUM X-477

COLD-AIR PERFORMANCE EVALUATION OF A THREE-STAGE TURBINE HAVING A BLADE-JET SPEED RATIO OF 0.156 DESIGNED FOR A 100,000-POUND-THRUST HYDROGEN-OXYGEN ROCKET TURBOPUMP APPLICATION*

By Milton G. Kofskey

SUMMARY

A three-stage turbine designed to power the propellant pumps of a 100,000-pound-thrust hydrogen-oxygen rocket stage was investigated experimentally with cold air.

Three-stage static efficiency was 0.65, and the equivalent specific work was 34.6 Btu per pound at design speed and an inlet-total to exit-static pressure ratio of 7.02. The total efficiency at design blade-jet speed ratio of 0.156 was 0.71. This results from experimental stage total efficiencies of 0.68, 0.66, and 0.69 in the first, second, and third stages, respectively. First-stage performance indicated a total efficiency of 0.68 and equivalent specific work of 11.7 Btu per pound at design speed and first-stage pressure ratio. Two-stage total efficiency and work at design speed and two-stage pressure ratio were, respectively, 0.69 and 22.8 Btu per pound. First-stage, two-stage, and three-stage performance indicated good agreement with design values of efficiency and equivalent specific work.

INTRODUCTION

The turbine research program at the NASA Lewis Research Center includes the study of turbines for various rocket propellant pump-drive applications. One type of pump-drive turbine that is of interest is for a bleed-type hydrogen-oxygen rocket application. The design blade-jet speed ratios for these turbines are low because of the high energy content of the hot hydrogen and steam relative to blade speeds that are limited by the conditions of temperature and stress. It is desirable to

*Title, Unclassified.

DECLASS

[redacted]

obtain high turbine efficiencies in order to minimize the amount of bleed flow and hence minimize the loss in specific impulse based on total propellant flow. Studies such as those of reference 1 have shown that multistage turbines are required for high efficiencies in the low blade-jet speed ratio range.

A three-stage turbine with a blade-jet speed ratio of 0.156 was designed to meet the requirements of a bleed-type turbopump for a 100,000-pound-thrust hydrogen-oxygen rocket in order to obtain the experimental performance level of this type of multistage turbine. The turbine was operated with air at inlet conditions of 710° R and 50 inches of mercury absolute.

This report presents the turbine performance and includes detailed information on the design loss assumptions, velocity diagram calculation, and blade design. The experimental results include first-stage, two-stage, and three-stage performance over a range of speeds and pressure ratios.

SYMBOLS

A_{an}	turbine-exit annular area, sq ft
c_p	specific heat at constant pressure, Btu/(lb)(°R)
D_p	pressure-surface diffusion parameter, $1 - (V_{s,min}/V_i)$
D_s	suction-surface diffusion parameter, $1 - (V_e/V_{s,max})$
D_{tot}	sum of suction- and pressure-surface diffusion parameters, $D_p + D_s$
g	acceleration due to gravity, 32.17 ft/sec^2
Δh	specific enthalpy drop, Btu/lb
J	mechanical equivalent of heat, 778.2 ft-lb/Btu
l	length of blade mean camber line, ft
p	absolute pressure, lb/sq ft
R	gas constant, ft-lb/(lb)(°R)
T	absolute temperature, °R
U	mean blade velocity, ft/sec

E-1370

V absolute gas velocity, ft/sec

V_j ideal jet speed corresponding to total-to-static pressure ratio,

$$\sqrt{2gJc_pT_i'\left[1 - \left(\frac{p_e}{p_i}\right)^{\frac{\gamma-1}{\gamma}}\right]}, \text{ ft/sec}$$

W relative gas velocity, ft/sec

w weight-flow rate, lb/sec

α absolute gas flow angle measured from axial direction, deg

γ ratio of specific heats

δ ratio of inlet pressure to NACA sea-level pressure, $p_i'/2116.2$

ϵ function of γ used in relating weight flow to that using inlet conditions at NACA standard sea-level atmosphere,

$$\epsilon = \frac{0.740}{\gamma}\left(\frac{\gamma + 1}{2}\right)^{\frac{\gamma}{\gamma-1}}$$

η total efficiency, based on total-to-total pressure ratio across turbine

η_s static efficiency, based on total-to-static pressure ratio across turbine

Θ_{cr} squared ratio of turbine-inlet critical velocity to that of NACA standard sea-level atmosphere, $\left(\frac{V_{cr}}{1019}\right)^2$

θ momentum thickness, ft

ν ratio of blade-jet speed, U/V_j

Subscripts:

an annular

cr conditions corresponding to Mach number of 1

e exit to blade row

i inlet

max maximum

min minimum

s surface

x axial component

Superscript:

' absolute total state

TURBINE DESIGN

As mentioned in the INTRODUCTION, the turbine design was based on the requirement of a bleed-system turbopump for a 100,000-pound-thrust hydrogen-oxygen rocket stage. The design requirements for the three-stage turbine having an 11.561-inch mean blade diameter are as follows:

Equivalent weight flow, $\epsilon \frac{w\sqrt{\Theta}}{\delta}$, lb/sec 1.017

Equivalent specific enthalpy drop, $\Delta h/\Theta_{cr}$, Btu/lb 34.92

Equivalent mean-radius blade speed, $U/\sqrt{\Theta_{cr}}$, ft/sec 253

Velocity Diagrams

The design velocity diagrams were calculated at the free-stream stations (fig. 1) for the mean blade radius to meet the design work requirements, and are based on the following assumptions:

(1) Rotor-inlet and -exit relative whirl components of equal magnitude

(2) Equal work split of 11.64 Btu/lb

As a first approximation, stage total efficiencies of 0.74, 0.72, and 0.72 were selected for stages 1, 2, and 3, respectively; these efficiencies were obtained from curves of reference 1. Velocity diagrams were calculated with these assumed efficiencies, and approximate stator and rotor blade profiles were drawn. Stator and rotor pressure losses were then calculated by the method of reference 2 using values from the velocity diagrams, blade profiles, and assigned ratios of momentum thickness to mean camber length. Figure 9 of reference 3 was used as a guide in assigning the ratio of momentum thickness to mean camber length. The calculated stator and rotor pressure losses then established the stage total efficiencies. The following table lists the ratios of momentum thickness to mean camber length assigned and the resulting design parameters:

Stage	Blade	θ_{tot}/l	Loss total-pressure ratio	Velocity coefficient, $\frac{V_{actual}}{V_{ideal}}$	Design p_i'/p_e (overall)	Stage total efficiency	Overall total efficiency
1	Stator	0.0035	0.945	0.956	1.825	0.70	0.70
	Rotor	0.020	0.884	0.823			
2	Stator	0.0070	0.920	0.917	3.415	0.65	0.68
	Rotor	0.020	0.870	0.824			
3	Stator	0.0070	0.900	0.912	7.02	0.67	0.71
	Rotor	0.020	0.880	0.820			

The ideal velocity term in the velocity coefficient corresponds to a velocity resulting from zero losses with the same area and exit static pressure used in determining the actual velocity. The overall static efficiency was 0.66. Free-stream velocity diagrams are shown in figure 2. From this figure, it can be seen that free-stream turning through the stators was 75.0°, 126.9°, and 122.0° for the first, second, and third stages, respectively. Free-stream turning through the rotors was 138.1°, 131.6°, and 121.1° in the first, second, and third stages, respectively. The figure also shows that the turbine was designed with an exit angle of approximately 43°.

Stator Design

The blade profiles were analyzed to obtain the blade surface velocities by using the method of reference 4, applied at the mean radius because of the high hub-tip radius ratio and constant blade profile from hub to tip.

The turbine annular area was increased to accommodate the pressure losses and maintain the prescribed velocity diagram. This was accomplished by increasing the blade height in equal amounts at the hub and tip to maintain the 11.561-inch mean diameter. The blade height from the exit of the first-stage stator to the inlet of the third-stage rotor was varied linearly from 0.341 to 0.715 inch. The design resulted in

120, 96, and 76 blades for the first to third stages, respectively, and blade solidities of 1.936, 1.681, and 1.833. Total diffusion D_{tot} for each stator was comparatively low, being 0, 0.357, and 0.399 for the first to third stages, respectively. Stator blade coordinates are given in table I(a).

Rotor Design

Rotor blade profiles determined at the mean radius were designed by the same method used in the stator design. Blade surface and mid-channel velocity distributions are presented in figures 3(d) to (f). Total diffusion D_{tot} for the rotors was 0.458, 0.327, and 0.607 for the first- to third-stage rotors, respectively. The design resulted in 159, 120, and 90 blades with solidities of 1.786, 2.346, and 1.985 for the first to third stages, respectively. The rotor blade height varied from 0.345 inch at the inlet to the first stage to 0.563 inch at the exit to the second-stage rotor. The blade height was constant at 0.715 inch for the third-stage rotor. Coordinates for the rotor blade profiles are given in table I(b).

E-1370

APPARATUS

The experimental investigation of the turbine was conducted in the same turbine test facility described in reference 5. The apparatus consisted of the turbine configuration, suitable housing to give uniform turbine-inlet flow conditions, and a cradled dynamometer to absorb turbine power output. A diagrammatic sketch of the turbine test section is shown in figure 4(a). Figures 4(b) to (d) show the three configurations investigated. A photograph of the three-stage rotor is shown in figure 5. The turbine was driven with dry pressurized air.

Stator blades ground from A-286 stainless-steel bar stock were located in slotted rings. The rotor blade passages in the Inconel 700 steel blanks were made by an electric-arc destruction method.

The rotor blade tip clearances were 0.014 inch for the first stage and 0.015 inch for the second and third stages. A nominal axial clearance of 0.019 inch between stator and rotor was used for all three stages.

In order to minimize leakage between stages, labyrinth-shaft seals were used on the second- and third-stage stators. The seals were located on a 5-inch diameter, and clearance between the seal and the rotor hub was 0.015 inch.

INSTRUMENTATION

The actual specific work output was computed from weight flow, torque, and speed measurements. The weight flow was measured with a calibrated ASME flat-plate orifice. The turbine output torque was measured with a commercial self-balancing torque cell and a mercury manometer. Turbine rotative speed was measured with an electronic events-per-unit-time meter.

Stator-exit static pressures were measured from three static-pressure taps spaced 120° apart on the outer wall immediately downstream of the stator blades (stations 1 to 5, fig. 1). Each pressure tap was centrally located in the projected stator flow passage.

Turbine-inlet measurements were taken in the annulus upstream of the stator inlet (station 0, fig. 4(a)). Three thermocouple total-pressure rakes were used for measurement of inlet total pressure and temperature.

Turbine-exit static pressures for each of the three series of tests were measured in the annulus, one axial chord length downstream of the rotor exit. Three static-pressure taps were spaced 120° apart on each of the inner and outer walls. Absolute rotor-discharge flow angle was measured with a two-tube wedge-type probe mounted in a self-alining actuator in the axial plane of the static-pressure measurements. Turbine-discharge temperature was measured with six thermocouple probes located downstream of flow-straightening vanes in the discharge ducting, approximately 2 feet downstream of the rotor exit.

EXPERIMENTAL PROCEDURE

The experimental investigation was conducted with a turbine-inlet temperature of 710° R and an inlet pressure of 50 inches of mercury absolute.

Performance data were obtained at turbine speeds of 70, 80, 90, 100, and 110 percent of design, and the exit static pressure was varied to give ratios of inlet-total to exit-static pressure from 1.5 to approximately 10. Performance data were obtained for first-stage, two-stage, and three-stage operation.

CALCULATIONS

The turbine was rated on the basis of the ratio of inlet-total to exit-static pressure and the ratio of inlet-total to exit-total pressure. The exit total pressure was calculated from weight flow, exit static pressure, exit total temperature, and flow angle from the following equation, which is a rearranged form of an equation (3) used in reference 6:

$$\frac{w\sqrt{T_e'}}{p_e A_{an} \cos \alpha_e} = \left[\frac{2\gamma g}{(\gamma - 1)R}\right]^{1/2} \left\{ \left[\left(\frac{p_i'}{p_e}\right)^{\frac{\gamma-1}{\gamma}} - 1\right] + \left[\left(\frac{p_i'}{p_e}\right)^{\frac{\gamma-1}{\gamma}} - 1\right]^2 \right\}^{1/2}$$

E-1370

Turbine efficiency was calculated as the ratio of actual turbine work per pound weight flow to ideal work based on inlet temperature and over-all pressure ratio.

EXPERIMENTAL RESULTS

First-Stage Performance

The performance of the first stage of the three-stage turbine is presented in figure 6. In this figure, equivalent weight flow $\epsilon \frac{w\sqrt{\Theta}}{\delta}$, equivalent specific work output $\Delta h/\Theta_{cr}$, and total efficiency η (based on total-to-total pressure ratio) are plotted against the ratio of inlet-total to exit-static pressure for turbine speeds of 70 to 110 percent of design speed. Total efficiency was computed because, in a multistage turbine, the kinetic energy at the exit of each stage except the last is available for the following stage.

At design pressure ratio (1.82) and design speed, the total efficiency was 0.68 and the equivalent specific work was 11.7 Btu per pound. This compares favorably with design equivalent work of 11.6 Btu per pound and total efficiency of 0.70. The occurrence of the specific work greater than design and a total efficiency less than design stems from the fact that, at design total-to-static pressure ratio, the total-to-total pressure ratio was greater than design, which results in the reduction in total efficiency. In other words, experimental and design inlet-total to exit-total pressure ratios would not be the same for values of efficiency and work being compared. Equivalent weight flow was 0.989, which is approximately 2.8 percent below the design value of 1.017 pounds per second. Figure 6(a) shows that for pressure ratios over 2.5 the stator was choked and, as a result, the equivalent weight flow was constant for all speeds.

Two-Stage Performance

The performance of the first two stages of the three-stage turbine is presented in figure 7. Equivalent specific work output and total efficiency are plotted against the ratio of inlet-total to exit-static pressure. At design pressure ratio (3.42), the total efficiency was 0.69 and the equivalent specific work was 22.8 Btu per pound. This compares favorably with the design values of 0.68 and 23.2.

Equivalent weight flow at design speed and pressure ratio was 1.000, which is 1.7 percent below the design value of 1.017 pounds per second. Figure 7(a) shows a variation of weight flow with turbine speeds for all pressure ratios; this indicates that the second stage is choked for pressure ratios above 5.5.

Three-Stage Performance

Overall performance of the three-stage turbine is presented in figure 8, where the performance parameters are plotted against ratio of inlet-total to exit-static pressure for turbine speeds of 70 to 110 percent of design speed. The figure shows that, at design pressure ratio (7.02) and speed, the total efficiency was 0.71 and the equivalent specific work was 34.6 Btu per pound. This agrees closely with the design efficiency of 0.71 and equivalent specific work of 34.9 Btu per pound. The curves of equivalent specific work against pressure ratio show that the turbine was conservatively designed in that the design point was not near limiting loading. Figure 8(a) shows that the weight flow at design pressure ratio and speed was 0.995, which is 2.2 percent below the design value of 1.017 pounds per second. The variation in equivalent weight flow with speed indicates that the third-stage stator or rotor was choking.

Figure 9 presents the variation of static efficiency with the ratio of inlet-total to exit-static pressure and with blade-jet speed ratio. Static efficiency is plotted because the kinetic energy is not recovered at the turbine exit of the last stage. Figure 9(a) shows that, at design pressure ratio (7.02) and speed, the static efficiency was 0.65, which agrees closely with a design efficiency of 0.66. Figure 9(b) shows the variation of static efficiency over the range of speeds and blade-jet speed ratios. The comparative flatness of the curves shows that the turbine was not operating near limiting loading. The trend of the curves also indicates that a single line drawn along the peak of the curves could be used for correlation of turbine performance data over most of the operating range covered.

Figure 10 gives a comparison of the design and the experimentally obtained static-pressure variation through the turbine. This figure was used in conjunction with the performance curves of the first stage and the first two stages in determining the stage work split at design overall pressure ratio and speed. The figure shows close agreement at all stations except at station 3, which is at the discharge to the second-stage stator. The trend of pressure through the stator indicates that the throat area was too large, which resulted from the orientation-angle setting of the stator blades being smaller than design value.

Stage works were 12.0, 10.6, and 12.0 Btu per pound for the first, second, and third stages, respectively, compared with the design value of 11.6 in each stage. The overall experimental total efficiency of 0.71 therefore results from stage total efficiencies of 0.68, 0.66, and 0.69 in the first, second, and third stages, respectively.

The following table shows the first-, two-, and three-stage operation at design speed and pressure ratio:

[Design equivalent weight flow, 1.017 lb/sec.]

Configuration	Experimental equivalent weight flow, lb/sec	Design equivalent specific work, Btu/lb	Experimental equivalent specific work, Btu/lb	Design efficiency	Experimental efficiency
First stage	0.989	11.6	11.7	0.70	0.68
Two stage	1.000	23.2	22.8	.68	.69
Three stage	.995	34.9	34.6	.71 [a].66	.71 [a].65

[a]Static efficiency.

Performance Comparison

Cold-air performance of a three-stage turbine designed for a similar hydrogen-oxygen turbopump rocket application, but of lower thrust, is presented in reference 7. The overall static efficiency was 0.54 at a blade-jet speed ratio of 0.135 as compared with a static efficiency of 0.65 and a blade-jet speed ratio of 0.156 for the subject turbine. In order to determine why the reference turbine had a lower efficiency, the following section presents a comparison of the design factors that could have contributed to a lower efficiency.

As mentioned previously, the design point was near limiting loading. The absolute exit velocity was 0.83, as compared with 0.52 for the subject turbine. This difference in exit velocity corresponds to approximately 4 points in static efficiency. The difference in blade-jet speed ratio for the two turbines would result in an additional 4 points in efficiency. Therefore, the reference turbine would have a static efficiency of approximately 0.62 if designed for the same conditions of blade-jet speed ratio and absolute discharge velocity of the subject turbine. Since the blade heights of the reference turbine were smaller than those of the subject turbine, increased loss due to tip clearance would account for part of the remaining difference in efficiency. A tip clearance investigation reported in reference 8 indicated that there was a 1.75-percent decrease in turbine work for every increase in tip clearance of 1 percent of annular passage height. Therefore, the effective greater tip clearance for the reference turbine accounted for approximately 1.7 points in efficiency. Increased interstage seal losses, blockage, and high blade loading in the second- and third-stage rotors could account for a large part of the remaining difference in static efficiency.

E-1370

SUMMARY OF RESULTS

Results of the cold-air investigation of an 11.561-inch-mean-diameter three-stage turbine can be summarized as follows:

1. At design speed and total-to-static pressure ratio, performance of the first stage showed that the total efficiency was 0.68 and the equivalent specific work was 11.7 Btu per pound. This is in close agreement with the design values of 0.70 and 11.6 Btu per pound.

2. Performance of the first two stages at design speed and total-to-static pressure ratio showed that the total efficiency was 0.69 and equivalent specific work was 22.8 Btu per pound. These values show good agreement with the design values of 0.68 and 23.2 Btu per pound.

3. Three-stage performance at design speed and total-to-static pressure ratio showed that the equivalent specific work was 34.6 Btu per pound and the total efficiency was 0.71. Comparison with design values of 34.9 Btu per pound and 0.71 in efficiency indicates that design conditions were obtained experimentally. At this point, a static efficiency of 0.65 was obtained, which compares closely with the design value of 0.66.

4. Three-stage performance at design speed and total-to-static pressure ratio showed that the equivalent weight flow was 0.995, which is 2.2 percent below the design value of 1.017 pounds per second.

5. The experimental work split for three-stage operation at design speed and overall pressure ratio was 12.0, 10.6, and 12.3 Btu per pound with total efficiencies of 0.68, 0.66, and 0.69 for the first, second, and third stages, respectively. This deviation from the design equal work distribution occurred primarily because the throat area of the second-stage stator was somewhat larger than design.

Lewis Research Center
National Aeronautics and Space Administration
Cleveland, Ohio, September 11, 1961

E-1370

REFERENCES

1. Stewart, Warner L.: Analytical Investigation of Multistage-Turbine Efficiency Characteristics in Terms of Work and Speed Requirements. NACA RM E57K22b, 1958.

2. Stewart, Warner L., Whitney, Warren J., and Miser, James W.: Use of Effective Momentum Thickness in Describing Turbine Rotor-Blade Losses. NACA RM E56B29, 1956.

3. Stewart, Warner L., Whitney, Warren J., and Wong, Robert Y.: A Study of Boundary Layer Characteristics of Turbomachine Blade Rows and Their Relation to Over-All Blade Loss. Paper 59-A-23, ASME, 1960.

4. Whitney, Warren J., Monroe, Daniel E., and Wong, Robert Y.: Investigation of Transonic Turbine Designed for Zero Diffusion of Suction-Surface Velocity. NACA RM E54F23, 1954.

5. Stewart, Warner L., Schum, Harold J., and Whitney, Warren J.: Investigation of Turbines for Driving Supersonic Compressors. I - Design and Performance of First Configuration. NACA RM E52C25, 1952.

6. Stewart, Warner L., Wong, Robert Y., and Evans, David G.: Design and Experimental Investigation of Transonic Turbine with Slight Negative Reaction Across Rotor Hub. NACA RM E53L29a, 1954.

7. Whitney, Warren J.: Cold-Air Investigation of a Three-Stage Turbine with a Blade- to Jet-Speed Ratio of 0.135 Designed for a 20,000-Pound-Thrust Hydrogen-Oxygen Rocket Turbopump Application. NASA TM X-414, 1960.

8. Kofskey, Milton G.: Experimental Investigation of Three Tip-Clearance Configurations Over a Range of Tip Clearance Using a Single-Stage Turbine of High Hub- to Tip-Radius Ratio. NASA TM X-472, 1961.

E-1370

TABLE I. - BLADE COORDINATES

(a) Stator

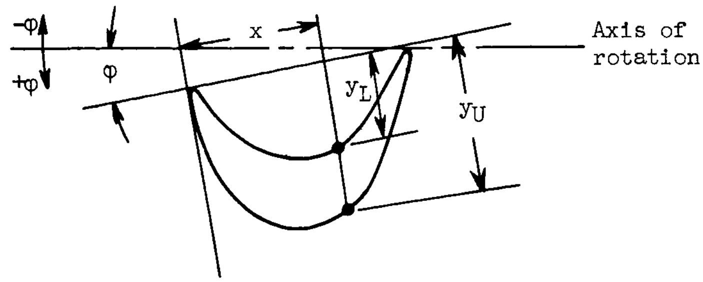

First stage			Second stage			Third stage		
Orientation angle, φ								
58°20'			19°30'			23°45'		
Average blade length, in.								
0.341			0.435			0.641		
Number of blades								
120			96			76		
x	y_U	y_L	x	y_U	y_L	x	y_U	y_L
0.000	0.040	0.040	0.000	0.006	0.006	0.000	0.009	0.009
.040	.095	.000	.025	.143	.037	.025	.195	.020
.050	.101	.001	.050	.257	.083	.050	.304	.063
.100	.116	.031	.100	.359	.145	.100	.396	.119
.150	.116	.052	.150	.403	.187	.150	.442	.158
.200	.109	.063	.200	.419	.213	.200	.466	.186
.250	.098	.066	.250	.419	.228	.250	.477	.204
.300	[a].085	.062	.300	.402	.232	.300	.476	.217
.350	-----	.055	.350	.369	.226	.350	.466	.225
.400	-----	.045	.400	.318	.211	.400	.447	.227
.450	-----	.033	.425	[a].285	.198	.450	.420	.224
.500	-----	.020	.450	-----	.184	.500	.385	.216
.550	-----	.008	.500	-----	.147	.550	.341	.204
.579	-----	.000	.550	-----	.097	.575	[a].317	.196
.586	.006	.006	.600	-----	.037	.600	-----	.187
			.631	-----	.000	.650	-----	.165
			.636	.005	.005	.700	-----	.137
						.750	-----	.103
						.800	-----	.062
						.850	-----	.015
						.876	.007	.007

[a]Straight line from this point to point of tangency with leading- or trailing-edge circle.

TABLE I. - Concluded. BLADE COORDINATES

(b) Rotor

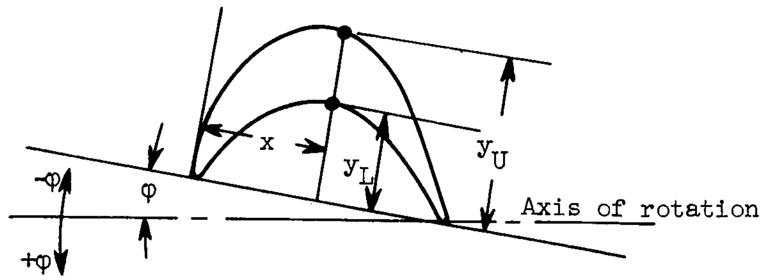

First stage			Second stage			Third stage		
Orientation angle, φ								
$-11^{\circ}43'$			$-10^{\circ}14'$			$-4^{\circ}17'$		
Average blade length, in.								
0.359			0.531			0.715		
Number of blades								
159			120			90		
x	y_U	y_L	x	y_U	y_L	x	y_U	y_L
0.000	0.008	0.008	0.000	0.008	0.008	0.000	0.006	0.006
.025	.150	.031	.025	.116	.025	.025	-----	.025
.050	.214	.070	.050	.202	.070	.050	.140	.061
.075	.247	.096	.100	.308	.134	.100	.250	.118
.100	.266	.114	.150	.368	.177	.150	.331	.159
.125	.276	.127	.200	.402	.207	.200	.385	.190
.150	.280	.136	.250	.419	.226	.250	.420	.214
.175	.278	.140	.300	.420	.236	.300	.441	.232
.200	.270	.141	.350	.411	.237	.350	.449	.241
.225	.255	.139	.400	.390	.230	.400	.448	.243
.250	.234	.133	.450	.356	.217	.450	.435	.239
.275	[a].204	.123	.500	.308	.194	.500	.410	.228
.300	-----	.109	.550	[a].244	.163	.550	.367	.210
.325	-----	.090	.600	-----	.120	.600	.304	.185
.350	-----	.065	.650	-----	.065	.625	[a].268	.170
.375	-----	.035	.710	.008	.008	.650	-----	.151
.408	.005	.005				.700	-----	.107
						.750	-----	.051
						.801	.009	.009

[a]Straight line from this point to point of tangency with leading- or trailing-edge circle.

E-1370

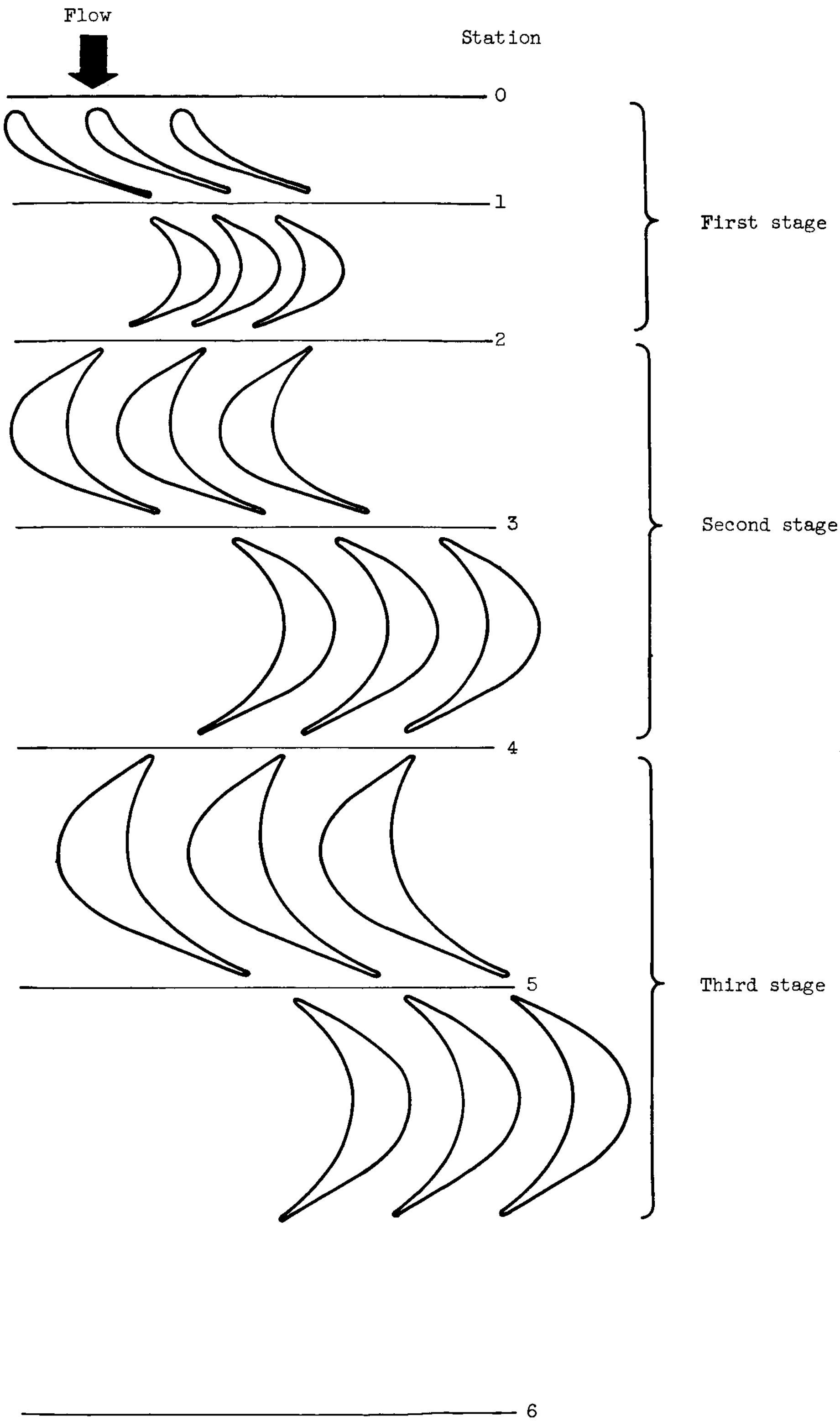

Figure 1. - Stator and rotor blade passages and profiles.

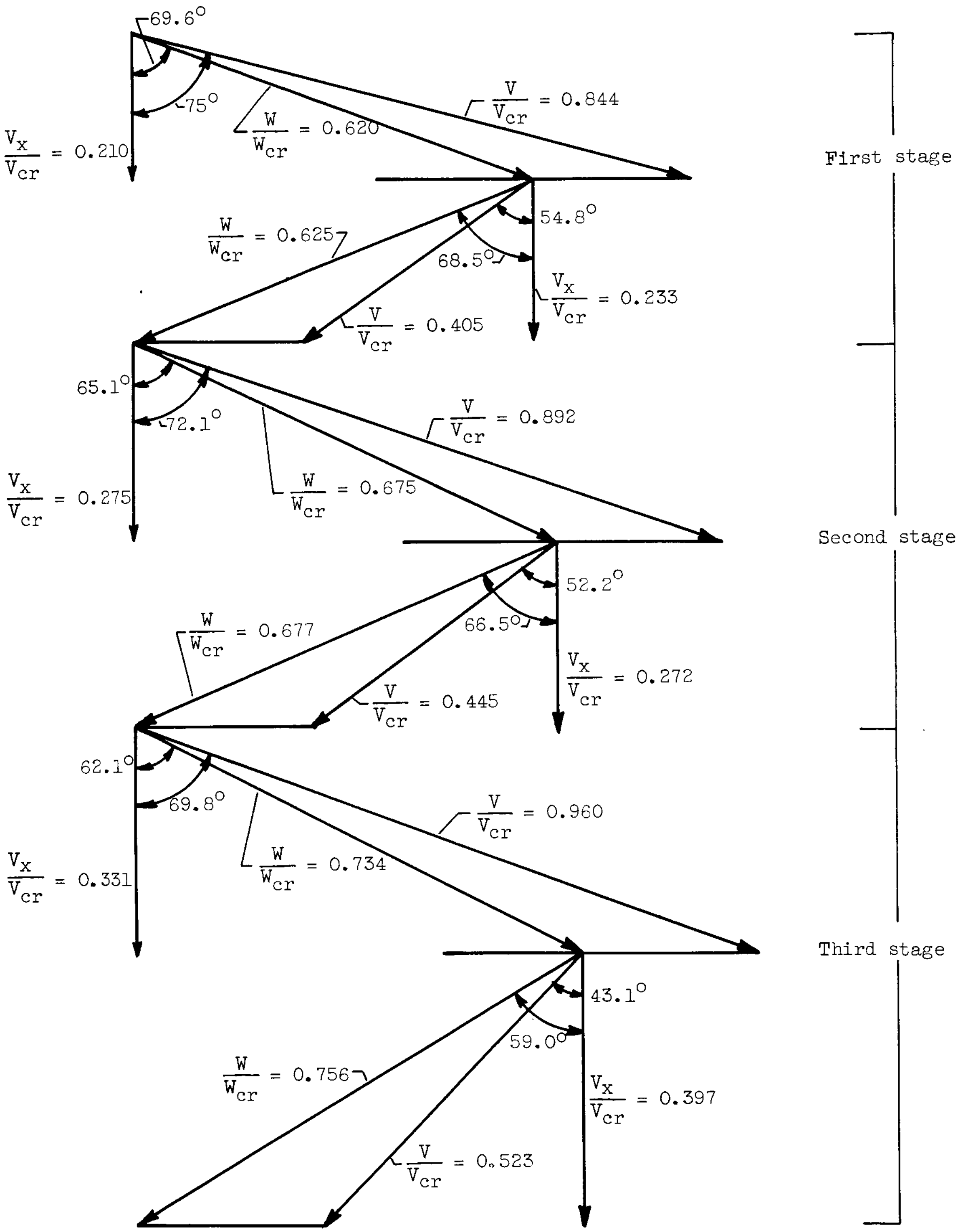

Figure 2. - Design mean-radius free-stream velocity diagram.

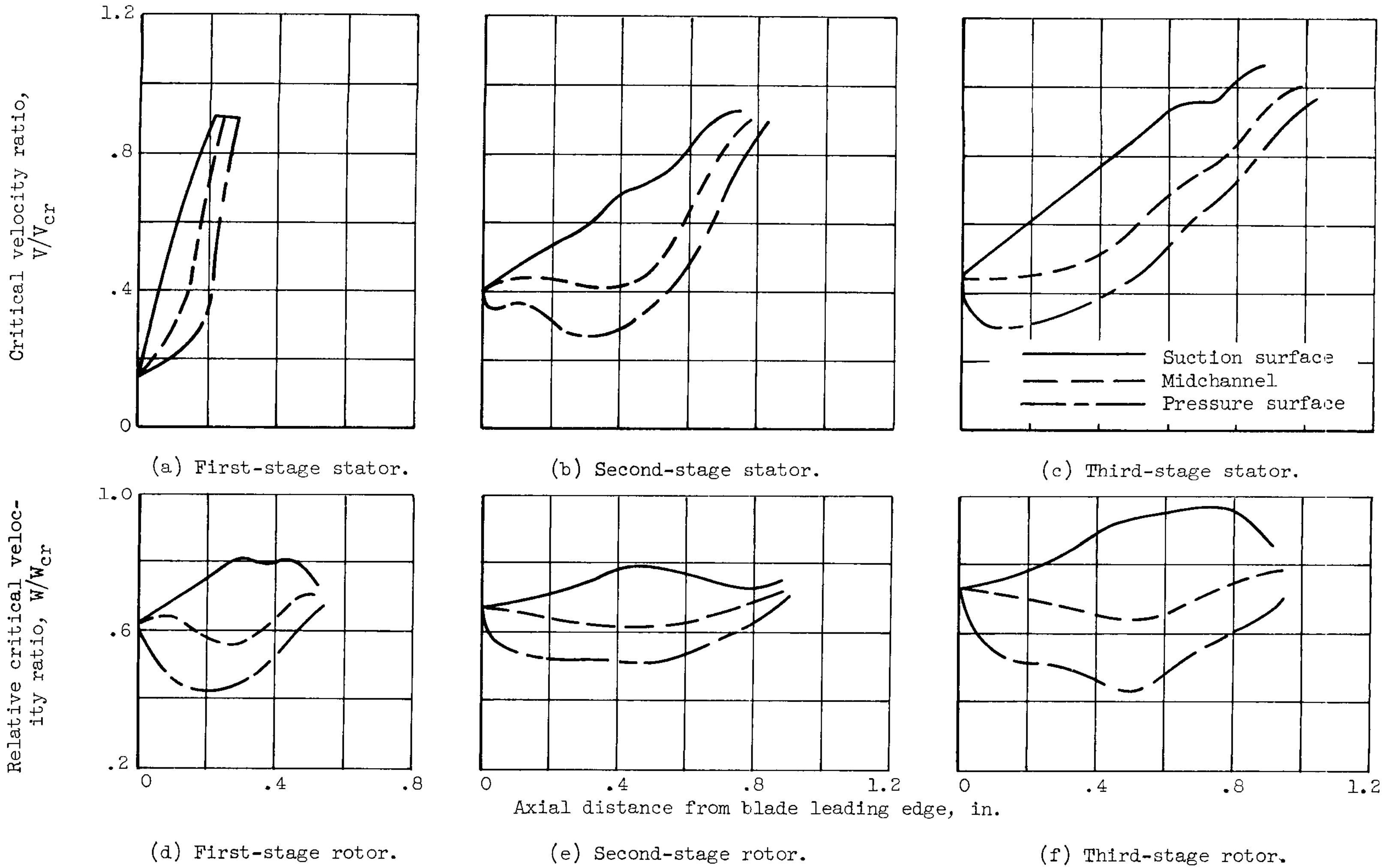

Figure 3. - Design midchannel and blade surface velocity distributions at mean radius.

E-1370

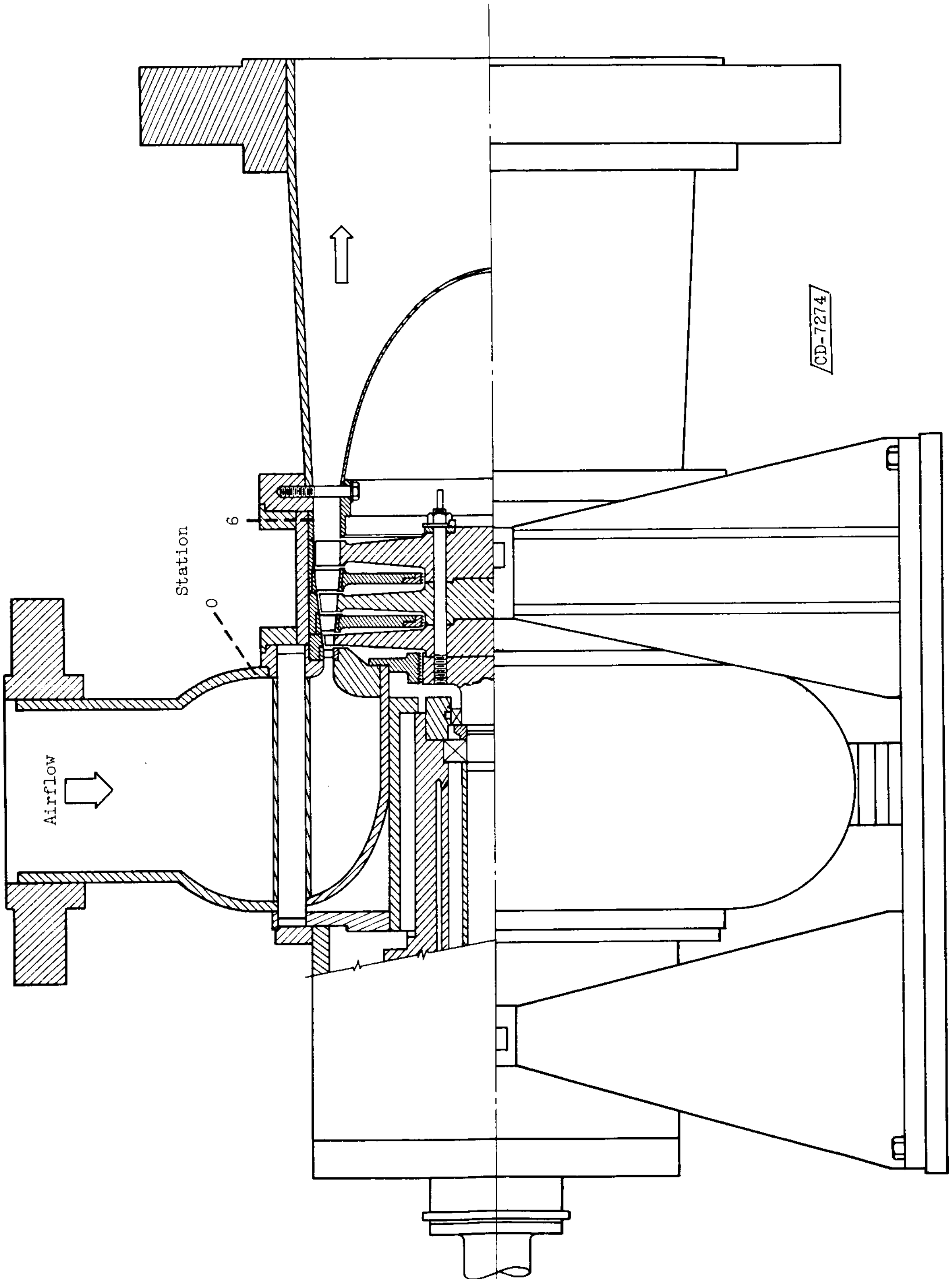

(a) Overall view.

Figure 4. - Turbine test section.

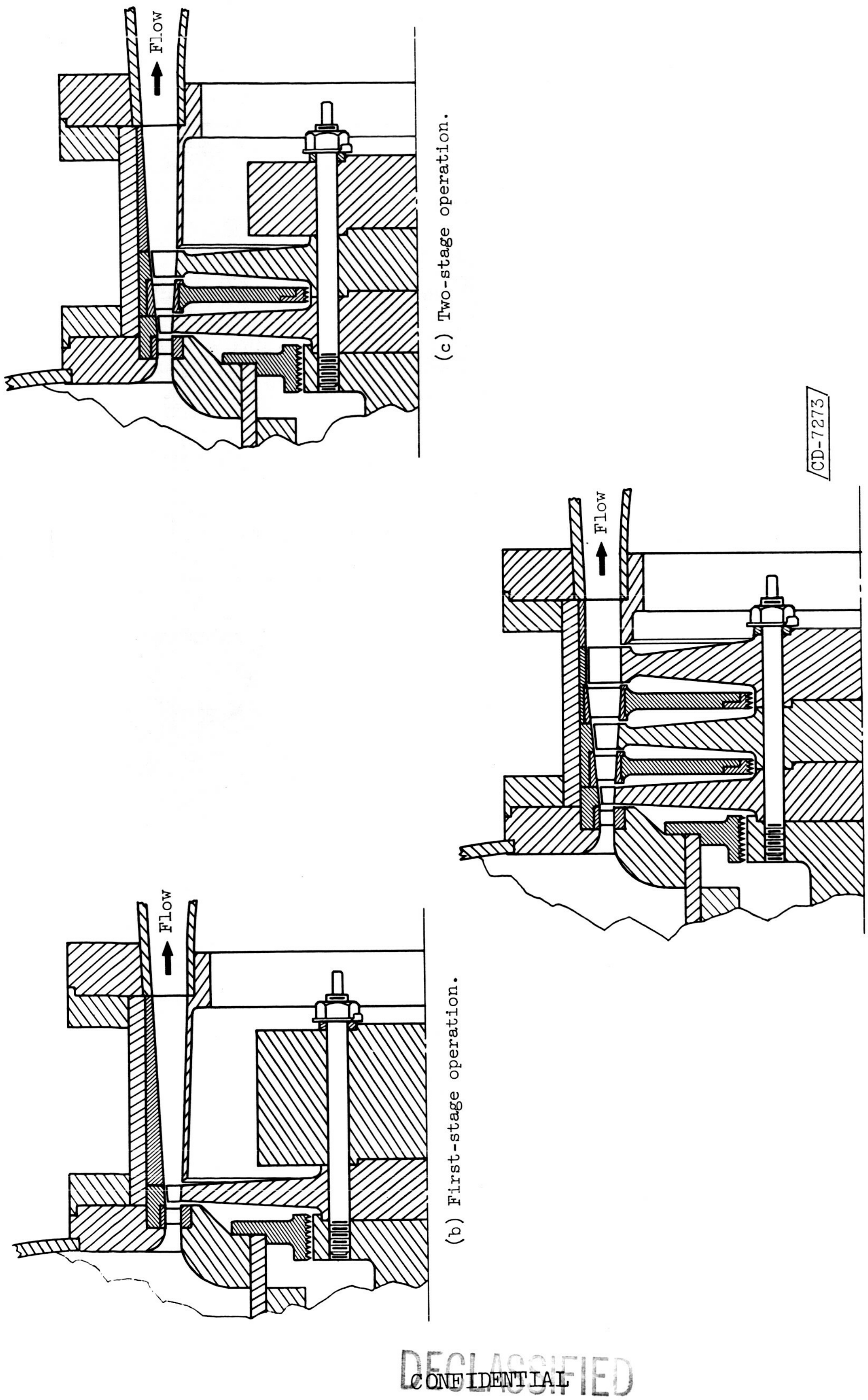

(b) First-stage operation.

(c) Two-stage operation.

(d) Three-stage operation.

Figure 4. - Concluded. Turbine test section.

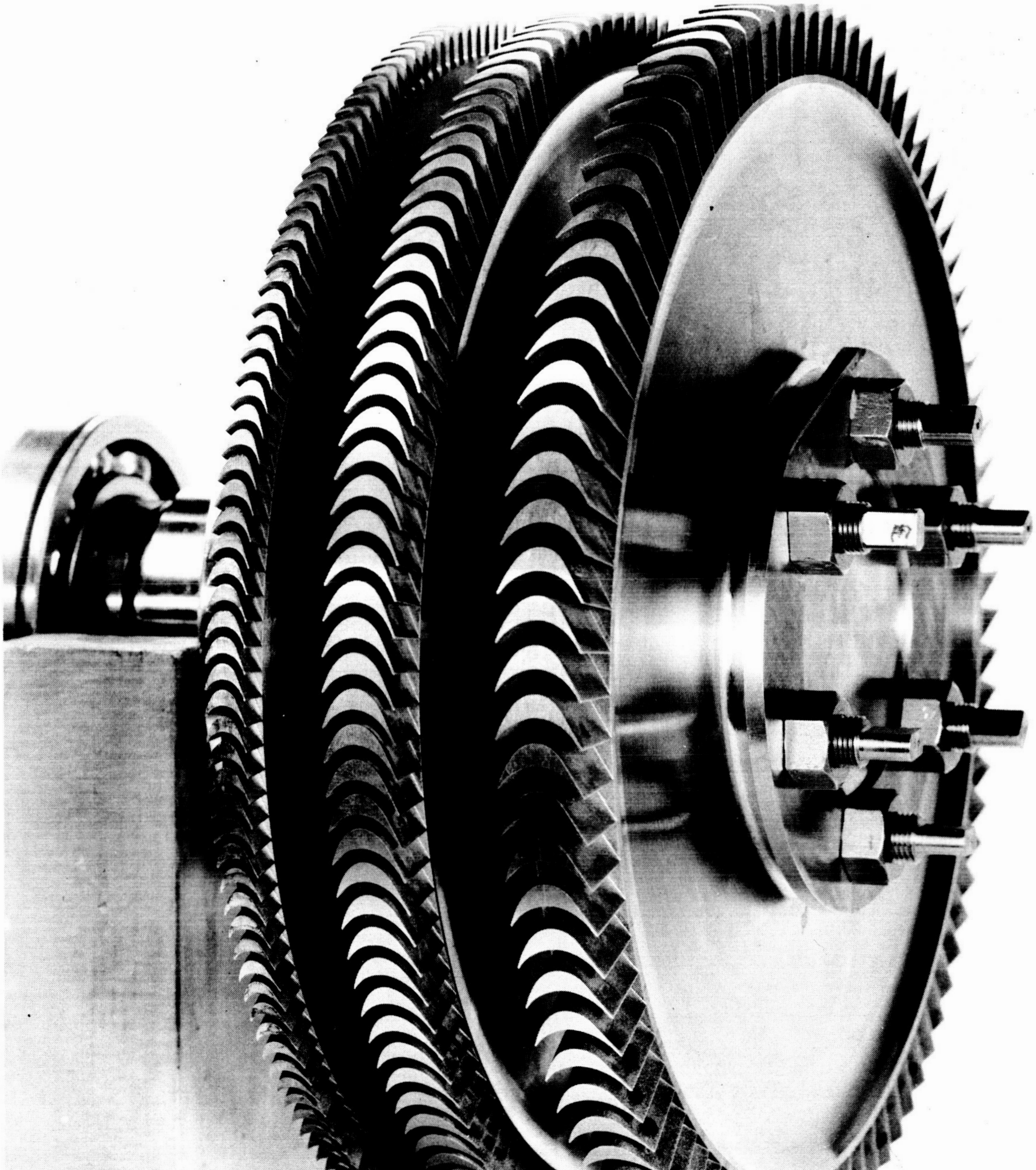

C-54613

Figure 5. - Three-stage turbine rotor.

E-1370

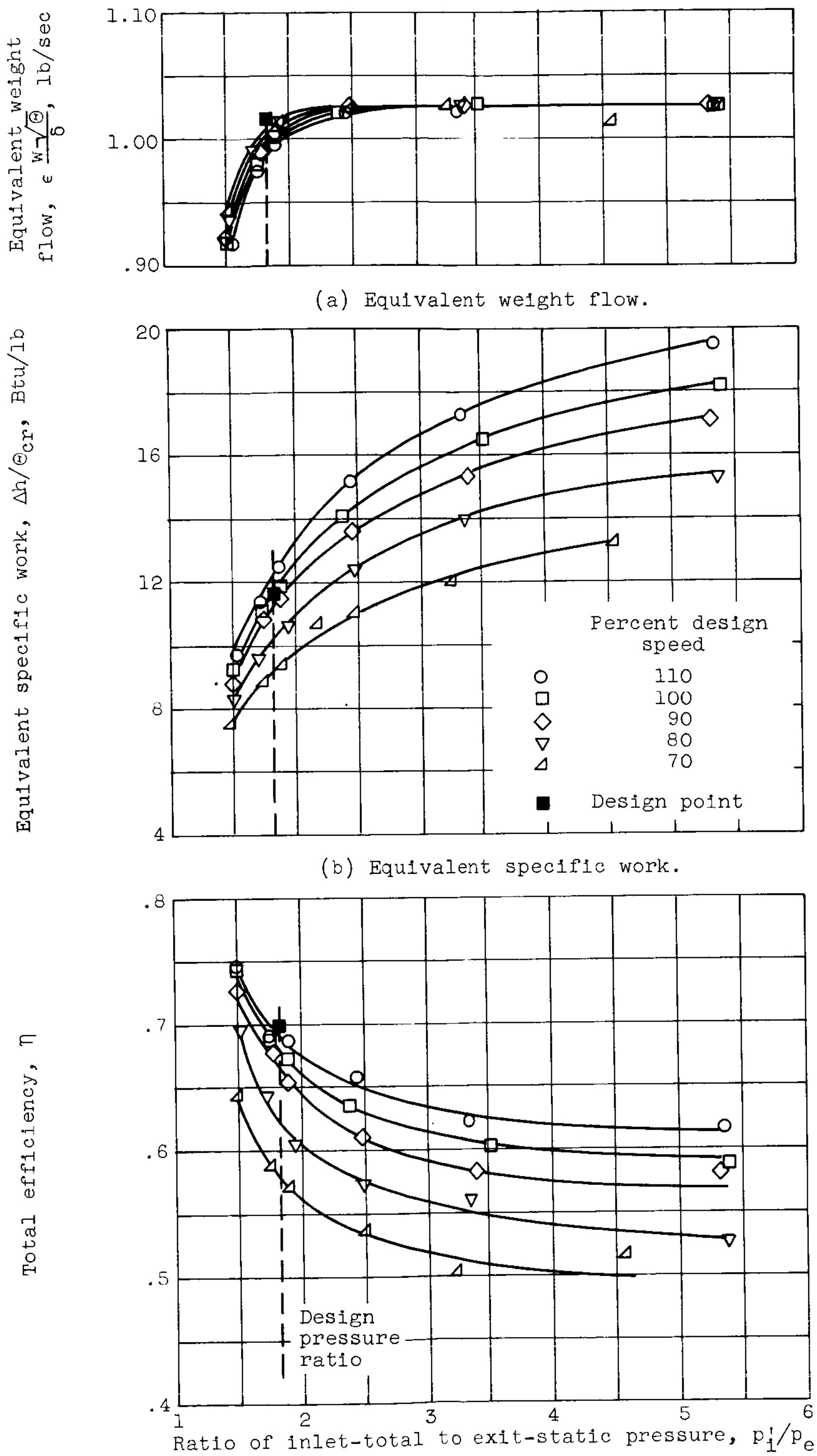

Figure 6. - Experimental first-stage performance of three-stage turbine.

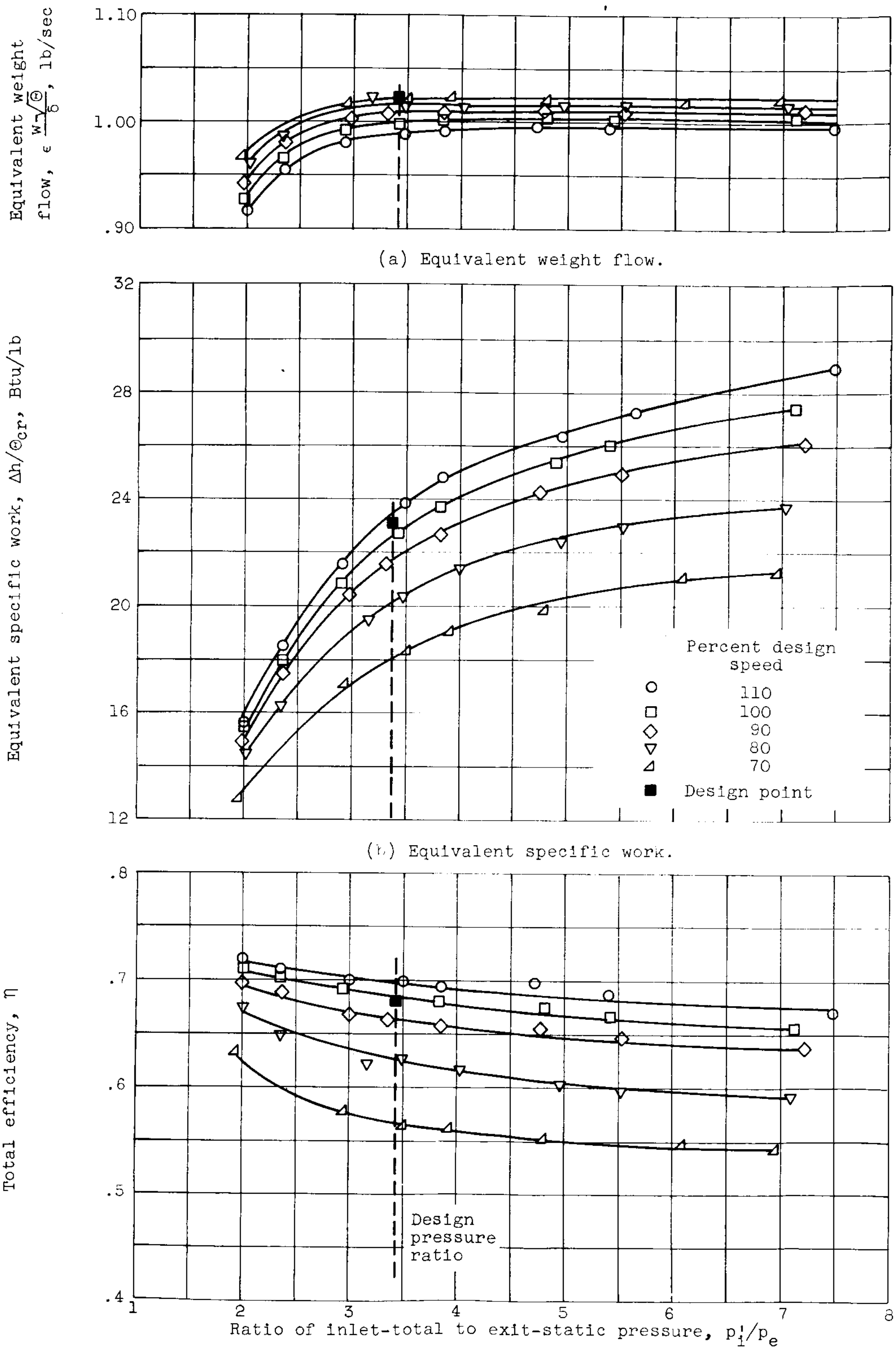

(a) Equivalent weight flow.

(b) Equivalent specific work.

(c) Turbine efficiency.

Figure 7. - Experimental two-stage performance of three-stage turbine.

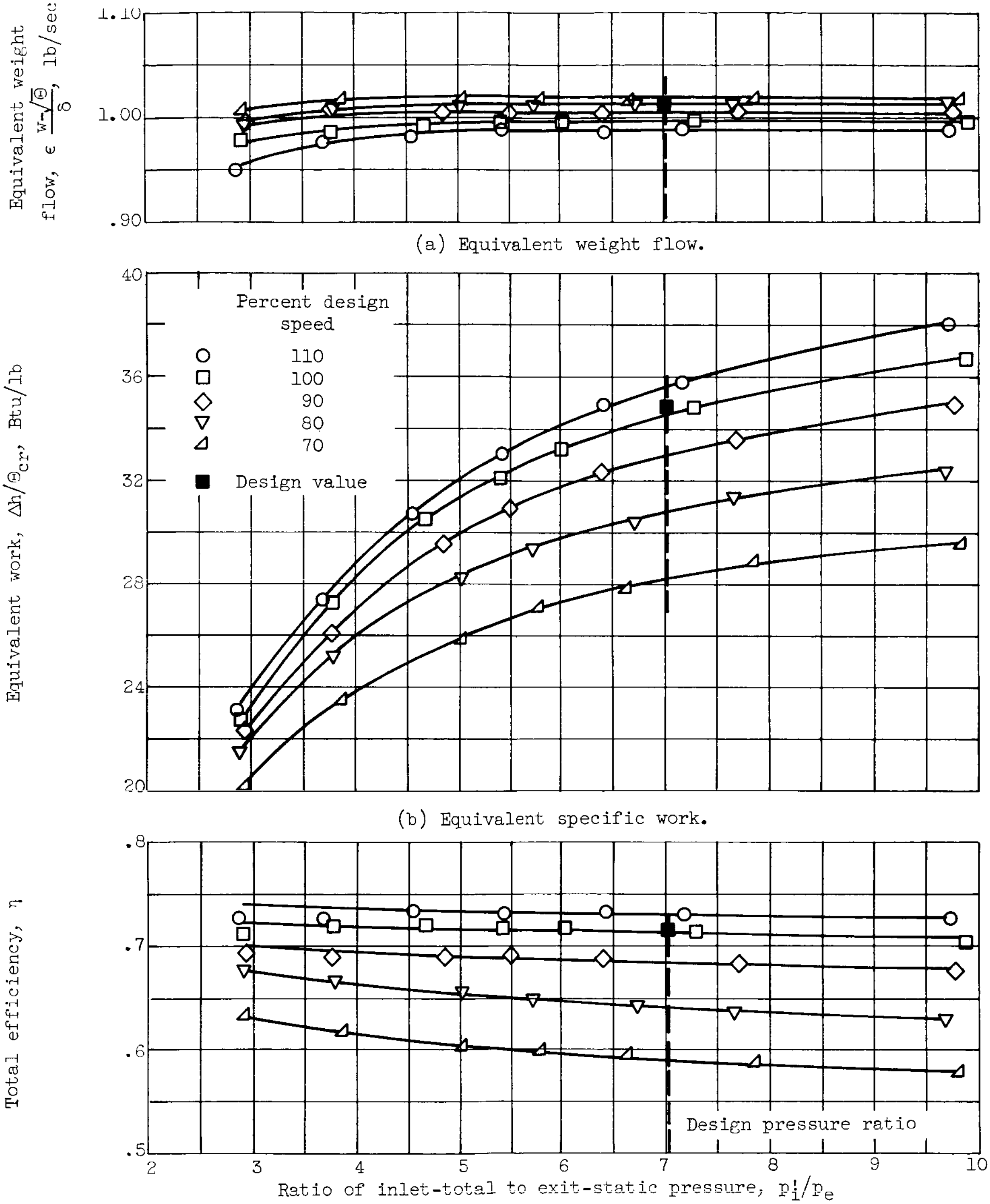

(c) Turbine efficiency.

Figure 8. - Three-stage performance of three-stage turbine.

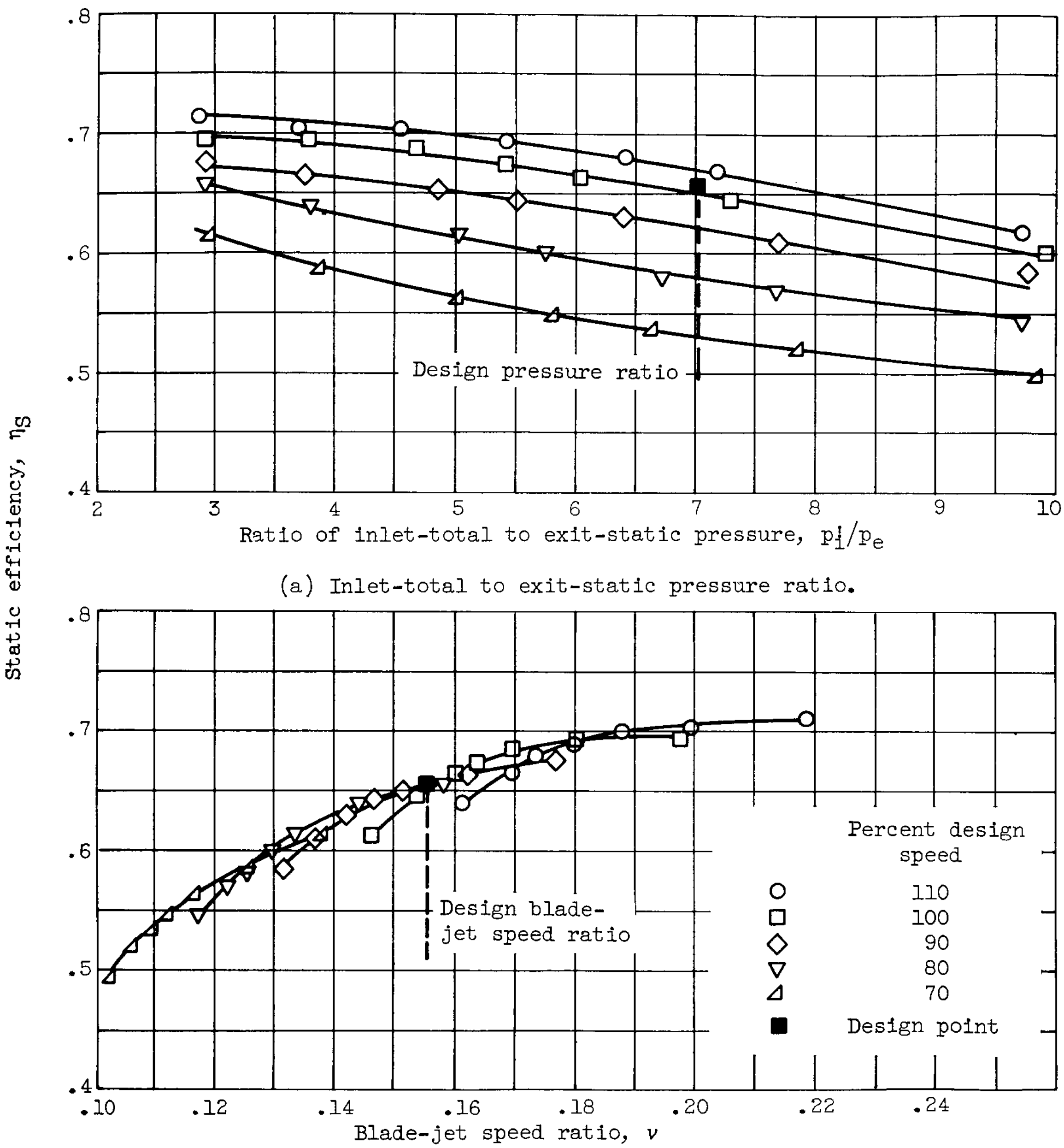

(a) Inlet-total to exit-static pressure ratio.

(b) Blade-jet speed ratio.

Figure 9. - Overall three-stage turbine efficiency.

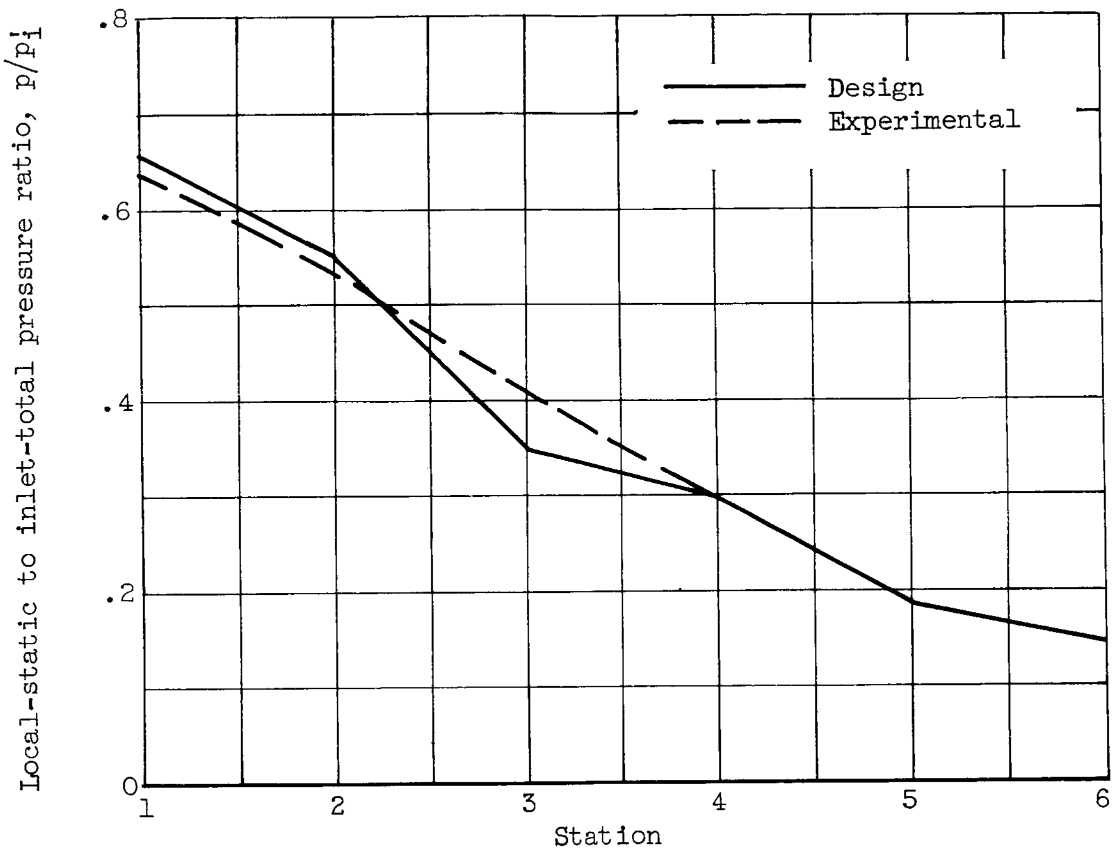

Figure 10. - Comparison of design and experimental static-pressure variation.